CWE-8
June 7-11, 2026
London, ON, Canada

Effectiveness of Wall-Modeled Large-Eddy Simulation in Simulating Tornado-Like Vortices

Anamika Malla[a], *Hui Zhang*[b], *Delong Zuo*[c]

a Texas Tech University, Lubbock, Texas, USA, a.malla@ttu.edu
b Texas Tech University, Lubbock, Texas, USA, huizhang@hotmail.com
c Texas Tech University, Lubbock, Texas, USA, Delong.Zuo@ttu.edu

SUMMARY
Wall-modelled large-eddy simulation (WMLES) can provide a computationally efficient alternative to wall-resolved LES (WRLES) for high-Reynolds-number flows, but its effectiveness in simulating tornado-like vortices is uncertain as, the near-ground flow region exhibits strong adverse pressure gradients. This study presents WMLES of tornado-like vortices generated in a Ward-type simulator at two swirl ratios and evaluates its performance against a high-fidelity WRLES reference. Simulated velocity and surface pressure fields are compared against laboratory measurements across all three LES configurations. The results show that while WMLES reproduces the mean vortex structure with reasonable fidelity, it overpredicts near-core pressure fluctuations and fails to reproduce the turbulent character of tornado flow. Specifically, WMLES produces an artificially intense and vertically extended region of elevated velocity fluctuations absent in both the experiment and WRLES and cannot capture the near-floor distributions of skewness and kurtosis observed experimentally. These findings demonstrate that equilibrium wall functions are inadequate for accurate prediction of near-core pressure fluctuations and coherent vortex dynamics in tornado-like flows.
Keywords: Tornado-like vortices, Wall-modelled LES, Wall-resolved LES, near-ground flow fields, surface pressure.

1. INTRODUCTION

Tornadoes are one of the most destructive windstorms. With intense swirling flow, strong radial flow, and a large pressure deficit near the ground, the winds in tornadoes cause structural loads that differ fundamentally from those formed by conventional boundary-layer winds in both magnitude and spatial and temporal distributions (e.g., Haan Jr et al, 2010; Tang et al, 2018). Consequently, accurate characterization of near-ground tornado wind fields is essential for the design of tornado-resistant civil infrastructure. However, direct field measurements of wind within tornadoes remain inadequate for engineering applications, as existing observational datasets are often spatially incomplete and of low temporal resolution. In particular, measurements are rarely obtained within the lowest 50 m above ground level, the most critical region for structural loading (Kuai et al, 2008). Numerically produced tornado-like vortices of high temporal and spatially resolutions are therefore a valuable complement to experimental and observational studies of tornadoes.

Over the recent decades, numerical studies of tornado-like vortices have increasingly used large eddy simulation (LES) to investigate tornado vortex dynamics. These studies have successfully reproduced some key flow features of tornado-like vortices, such as the radial profile of mean tangential velocity and mean pressure deficit and the transition of the vortex from a single-celled structure to a two-celled structure with increasing swirl ratio (Bryan et al, 2017; Cao et al, 2018; Gairola and Bitsuamlak, 2019; Ishihara et al, 2011). The fidelity of such simulations, however, depends critically on how the near-ground flow region is treated. Two broad approaches have been used for near-ground treatment in LES. The first approach, known as wall-resolved LES

(WRLES), resolves the near-wall flow down to the viscous sublayer. It has been shown to accurately capture the near-surface momentum balance in tornado-like flows (Cao et al, 2018). However, this approach can be computationally expensive at high Reynolds numbers. The second approach, known as wall-modelled LES (WMLES), models the near-wall region with an algebraic equilibrium stress model and is a much more computationally efficient alternative to WRLES. WMLES has been shown to perform well for attached flows, including cases with complex geometries where accurate prediction is challenging (e.g., Bose and Park, 2018). A number of numerical simulations of tornado-like flow also employed the WMLES approach. For example, Ishihara et al. (2011) applied a law-of-the-wall function in the near-ground region where the near-wall mesh could not resolve the laminar sublayer. It was suggested that WMLES was employed because the radial pressure gradient dominates near the surface.

Despite the efficiency of WMLES, a factor that may limit its application in the simulation of tornado-like vortices is the presence of strong adverse pressure gradients and significant curvature of the flow, which fundamentally breaks the equilibrium assumption on which standard wall functions rely. For example, Gairola et al. (2024) showed that the boundary layer of tornado-like flow has strong streamwise variation in the pressure gradient and curvature that fundamentally distinguishes it from canonical flows for which standard wall models were developed. Additionally, Wang et al. (2023) demonstrated in an LES of atmospheric-scale tornado that the traditional equilibrium approach for modeling near-surface turbulence is not suitable for tornado flows. Yet no study has systematically evaluated the effectiveness of WMLES of tornado-like vortices with equilibrium wall functions against experiments or a WRLES reference.

The study aims to investigate the viability of WMLES with standard wall functions as a computationally efficient approach for simulating tornado wind fields. To achieve this goal, WMLES with standard wall function is employed to reproduce tornado-like vortices generated in the VorTECH tornado simulator at Texas Tech University. Some key characteristics of the simulated velocity and surface pressure fields are compared against experimental measurements. In addition, some results of the WMLES are also compared with those from a WRLES to illustrate the performances of these two types of simulations.

2. METHODOLOGY

2.1. VorTECH tornado simulator and numerical domain

The VorTECH is a Ward-type tornado simulator at Texas Tech University that can be used to generate tornado-like vortices of various mean and fluctuating flow characteristics. A description of the simulator can be found in Chen et al. (2023). In this study, LES is used to numerically reproduce vortices that are generated with the height of the confluence zone of the simulator set at 1 m, which gives an aspect ratio of 0.5, and the orientations of the turning vanes set at 25° and 30°, respectively, relative to the radial direction. According to experimental measurements, the swirl ratios of the physically generated vortices are 0.83 and 0.65, respectively. WMLES is used to reproduce both vortices by setting the height of the confluence zone and the orientations of the turning vanes the same as in the experiments; WRLES is used to reproduce the physically generated vortex with the turning vanes oriented at 25° relative to the radial directions only.

Figure 1(a) illustrates the computational domain for both types of simulations, which includes the turning vanes, confluence zone, updraft hole, and floor. The inlet is an annular plane at the base of the confluence zone where a swirling inlet velocity is applied. The outlet at the top of the updraft hole is specified as an open boundary with zero normal pressure gradient, permitting reverse flow that is needed for accurate reproduction of the downdraft observed in the center of the physically generated vortices. For WMLES, wall functions are applied on all solid surfaces, including the updraft hole walls, the top of the confluence zone, the floor, and the surfaces of the turning vanes. For WRLES, wall functions are also applied on these surfaces except for the floor. The meshes used for the WMLES and WRLES of the vortex with a swirl ratio of 0.65 differ only in the near-floor resolution. As an illustration, Figures 1(b) and 1(c) show the plan and elevation views of the computational mesh for the simulation of the vortex of swirl ratio 0.65. It consists of a fully structured hexahedral grid, with the mesh topology closely following the geometry of the simulator. The mesh resolution is refined in two regions. The first region is the near-wall layers adjacent to all solid boundaries and the second is the anticipated vortex core region, where strong radial pressure gradients and concentrated vorticity require higher spatial resolution to accurately capture the tornado flow structure. Table 1 summarizes some key characteristics of the meshes for WMLES of the vortices of swirl ratios 0.83 ("WMLES_083") and 0.65 ("WMLES_065") and WRLES of the vortex of swirl ratio 0.65 ("WRLES_065").

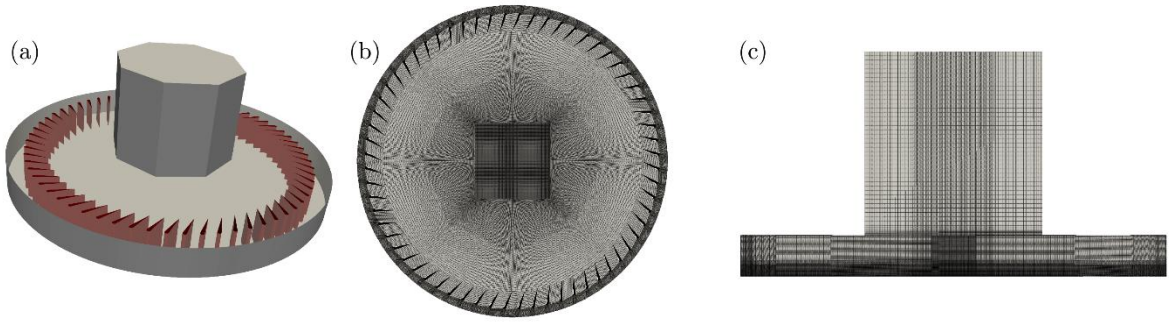

Figure 1: (a) Computational domain; (b) Top view of the structured mesh and (c) Plan view of the structured mesh.

Table 1. Parameters of simulation configurations.

Parameter	WMLES_083	WMLES_065	WRLES_065
Target Swirl ratio	0.83	0.65	0.65
Vane angle	30°	25°	25°
Floor wall treatment	Spalding's law	Spalding's law	Wall resolved
First cell height	0.0042 m	0.0032 m	3.2×10^{-5} m
Near-wall y^+	> 30	> 30	< 1
Inflation layers	—	—	26
Time step	1×10^{-4} s	1×10^{-4} s	7×10^{-5} s
Mesh count	11.2 million	24.6 million	47.3 million

2.2. Governing equations and turbulence modelling

The governing equations for the three-dimensional incompressible LES are the spatially filtered continuity and Navier–Stokes equations:

$$\frac{\partial u_i}{\partial x_i} = 0 \tag{1}$$

$$\frac{\partial u_i}{\partial t} + \frac{\partial \left(u_i u_j \right)}{\partial x_i} = -\frac{1}{\rho}\frac{\partial p}{\partial x_i} + \frac{\partial}{\partial x_j}\left(2\upsilon S_{ij} - \frac{\tau_{ij}}{\rho} \right) \tag{2}$$

where $u_i\,(i = 1, 2, 3)$ and p are the spatially filtered velocity components and pressure, respectively ρ is the air density, υ is the kinematic viscosity, and τ_{ij} is the subgrid-scale (SGS) stress tensor arising from the filtering operation. The filtered strain rate tensor of the resolved flow field is defined as:

$$S_{ij} = (1/2)(\partial u_i / \partial x_j + \partial u_j / \partial x_i) \tag{3}$$

In LES, spatial filtering distinguishes the large, energy-containing motions that are directly calculated on the grid from the smaller subgrid-scale motions, whose impacts on the resolved flow are modeled. The eddy-viscosity assumption is used to close the SGS stress is modeled as:

$$\tau_{ij} - \frac{1}{3}\tau_{kk}\delta_{ij} = -2\rho\upsilon_{sgs}S_{ij} \tag{4}$$

where, υ_{sgs} is the subgrid-scale turbulent viscosity. This study employs the *standard Smagorinsky model* with $\upsilon_{sgs} = (C_s\Delta)^2\left|S\right|$ where C_s is the Smagorinsky coefficient, $\Delta = (\Delta x\Delta y\Delta z)^{1/3}$ is the local filter width based on the grid cell volume, and $\left|S\right| = \sqrt{2S_{ij}S_{ij}}$ is the magnitude of the filtered strain rate tensor.

The standard Smagorinsky SGS model is selected based on Zhang (2024), which evaluated the performances of multiple SGS models in the simulations of tornado-like vortices and found the standard Smagorinsky turbulence model to perform the best. The Spalding's law (Spalding, 1961), which provides a unified description of the velocity profile across the viscous sublayer, buffer layer, and logarithmic region within a single continuous expression:

$$y^+ = u^+ + \frac{1}{E}\left[e^{ku^+} - 1 - ku^+ - \frac{1}{2}(ku^+)^2 - \frac{1}{6}(ku^+)^3 \right] \tag{5}$$

Where, $y^+ = yu_\tau / \upsilon$ is the dimensionless wall-normal distance, $u^+ = u / u_\tau$ is the dimensionless velocity, u_τ is the friction velocity, $k = 0.41$ is the von Kármán constant, and $E = 9.8$ is the wall roughness parameter. Equation (5) is a nonlinear implicit equation that is solved iteratively at each wall-adjacent cell to obtain u_τ, from which the wall shear stress $\tau_w = \rho u_\tau$ is computed and applied as a boundary condition. The Spalding's law is derived for fully developed flow under zero pressure gradient.

All simulations are performed in OpenFOAM, using the PISO algorithm for pressure–velocity coupling with two corrector steps per time step. Convective terms are discretized using a second-order central differencing scheme, and time integration employs a second-order implicit Crank–Nicolson scheme. The physical time step is set to $1\times10^{-4}s$ and $7\times10^{-5}s$ for the WMLES and WRLES configurations, respectively, ensuring that the Courant number does not exceed unity. The velocity and pressure of the flow resulting from the simulation were sampled at 625 *Hz*. The initial

10 *s* of data from each simulation is discarded to avoid the analysis being affected by transient effects, leaving 60 *s* of data for estimation of statistics.

3. RESULTS AND DISCUSSIONS

3.1. Mean Velocity Field

A comparison between the numerical results and the experimental measurements suggest that the numerical simulations perform reasonably well in reproducing the mean flow fields of the physically generated vortices. As an illustration, Figure 2 presents a comparison between some mean velocity profiles of the flows resulting from the numerical simulations with the corresponding measurements from the experiments ("S083": vortex of swirl ratio 0.83: "S065" vortex of swirl ratio 0.65). Here, $\overline{V}_\theta$ and $\overline{V}_r$ are the mean tangential and radial velocities, respectively. Also, $\overline{V}_{\theta,\max}$ is the maximum mean tangential velocity, r and z are radial distance from the vertical axis of the vortex and height above the floor, respectively, and r_c is the core radius of the specific vortex, which is the distance between the location of the maximum mean tangential velocity and the vertical axis of the vortex.

Figure 2(a) shows that all the numerically reproduced radial profiles of mean tangential velocity match the corresponding experimental profiles reasonably. It is noteworthy that for numerical simulations of the vortex of swirl ratio 0.65, the radial profile of the mean tangential velocity from WRLES matches the experimental profile better than that from the WMLES. Figure 2(b) suggests that the numerical simulations approximately reproduce the vertical profile of the mean radial velocity of the physically generated vortices. However, discrepancies between the experimental measurements and numerical results exist, especially at heights near where radial velocity of the maximum magnitude occurs. All three configurations capture the overall structure of the vertical velocity profile: strong inward radial velocity near the surface that decreases with height and approaches zero at $z / r_c \approx 0.5$ .The difficulty in reproducing radial velocity profiles has also been indicated in a number of previous studies, and one of the reasons for this difficulty was suggested to be the lack of resolved turbulence in prescribed inflow boundary conditions (Bryan et al, 2017; Liu et al, 2020).

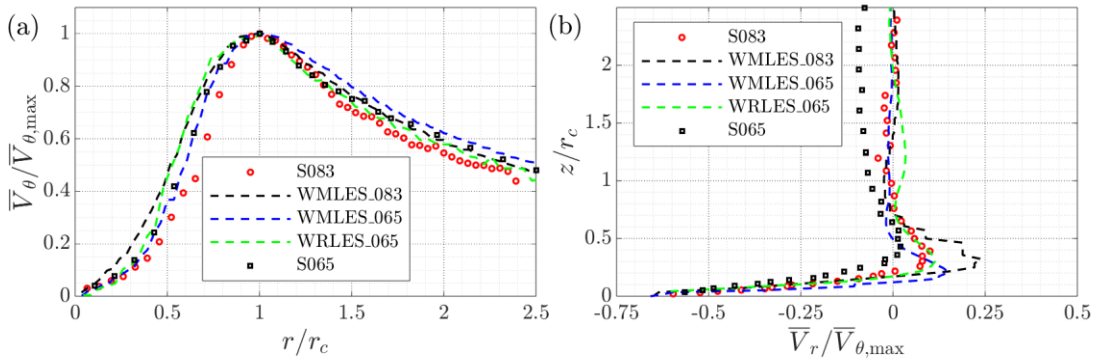

Figure 2: Mean velocity profiles of experimentally generated and numerically simulated vortices: (a) Radial profiles of mean tangential velocity at the height of maximum mean tangential velocity (b) vertical profiles of mean radial velocity at core radius.

3.2. Turbulent velocity field

A comparison between the numerically simulated vortices and physically generated vortices reveals the different performances of the two numerical approaches in reproducing the turbulence in the flow. As an example, Figure 3 shows a comparison of turbulence intensity of the tangential component of the flows (defined as $I_{v\theta} = \sigma_{V\theta} / \overline{V}_{\theta}$, where $\sigma_{V\theta}$ and $\overline{V}_{\theta}$ are the standard deviation and mean of the tangential component of the flow) resulting from WMLES and WRLES of the vortices of swirl ratio 0.65 with the corresponding turbulence intensity of the physically generated vortex. Due to the limitations of the Cobra probe used in the experiments, high frequency measurements of the flow velocity are only available over part of a vertical-radial plane. For this reason, Figure 3(a) shows turbulence intensity of this flow component only over the region where measurements are available, although Figure 3(b) and Figure 3(c) show the turbulence intensity over a much broader area. Both the experimental measurement and the numerical simulations suggest that over the region where experimental data is available, the tangential turbulence intensity increases as the flow approaches the center of the vortex from the inlet and turbulence of higher intensity occurs in regions near the floor. However, Figure 3 also suggests that the tangential turbulence intensity of the flow reproduced using WRLES matches the experimental measurements better than that reproduced using WMLES in both magnitude and spatial distribution. This is evidence of the limitation of WMLES in faithfully reproducing the turbulent characteristics of tornado-like vortices.

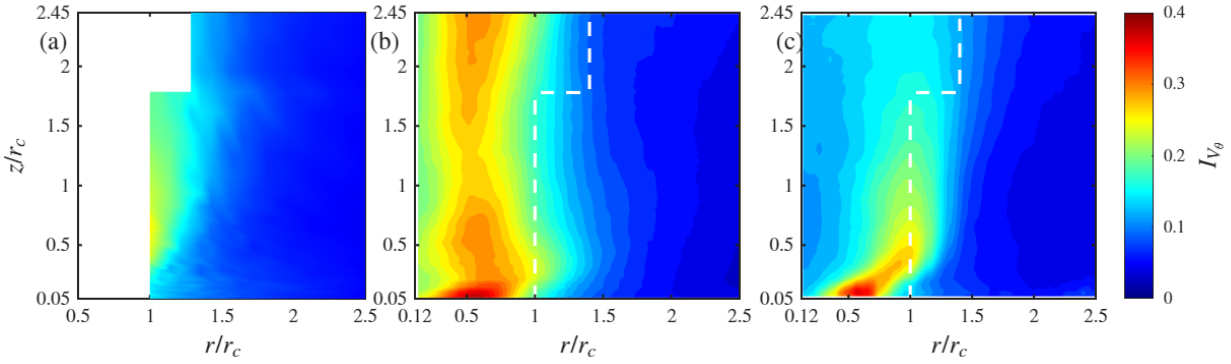

Figure 3: Turbulence intensity of tangential velocity in the *r*-*z* plane for (a) Experiment: S065, (b) WMLES_065 and (c) WRLES_065.

Figures 4 and 5 further compare the skewness and kurtosis, respectively, of the tangential components of the numerically simulated flows with those of the target physically generated vortex of swirl ratio 0.65. Both the numerical simulations and the experimental measurement suggest that the fluctuation of the tangential velocity can be significantly non-Gaussian, which, according to Tang et al (2025) is caused by the rotation of secondary vortices in the flow. However, it is apparent that these two moments of the turbulence produced by WRLES match the corresponding moments of the physically generated flow much better than the turbulence generated by WMLES. This is especially true in the region near the floor, where the skewness and kurtosis of the tangential velocity reproduced by WRLES resemble the corresponding moments of the tangential velocity generated by the simulator in both magnitude and spatial distribution. By contrast, the WMLES apparently underperforms in this region in reproducing the non-Gaussian characteristics of the turbulence.

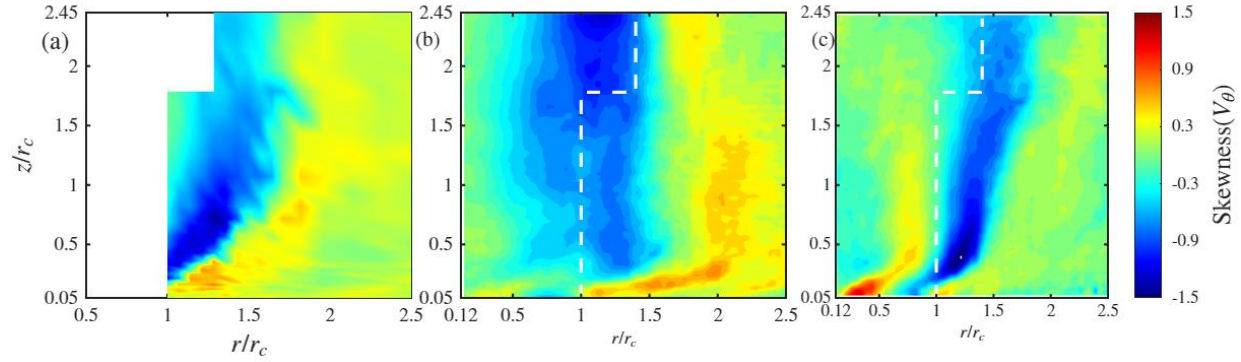

Figure 4: Skewness of the tangential velocity in the r-z plane for (a) Experiment: S065, (b) WMLES_065 and (c) WRLES_065.

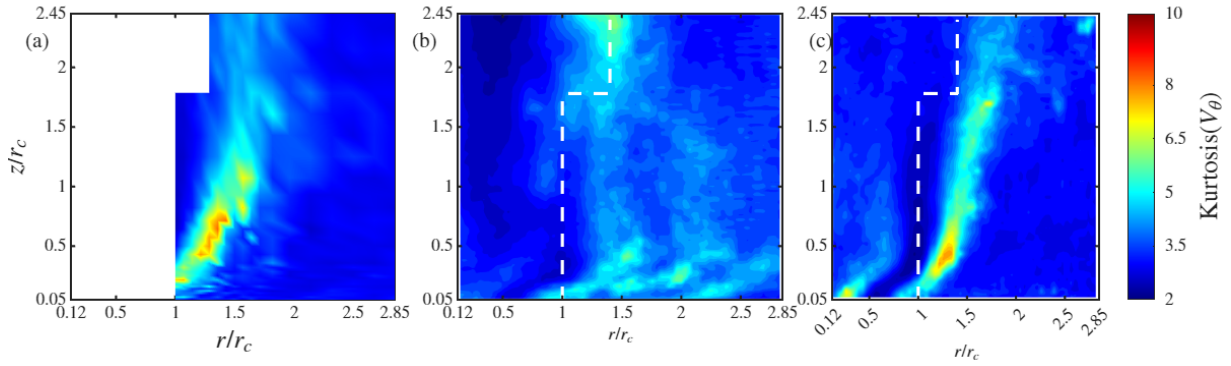

Figure 5: Kurtosis of tangential velocity in the r-z plane for (a) Experiment: S065, (b) WMLES_065 and (c) WRLES_065.

3.3. Characteristics of surface pressure

In addition to the different capabilities of the WMLES and WRLES in reproducing the characteristics of flow velocity, this study also revealed differences in the performances of these two types of numerical simulations in reproducing the characteristics of the pressure deficit caused by tornado-like vortices. As an example, Figure 6 compares radial profiles of the mean and standard deviation of the numerically reproduced surface pressures with the corresponding profile estimated based on the experimental measurements. Here, the surface pressure is represented by a pressure coefficient defined as: $C_p = (P - P_{ref}) / 0.5\rho(\overline{V}_{\theta,\max})^2$ where, P is the pressure at different radial locations and P_{ref} is taken at the pressure in the static bottle under the simulated floor for the experiments and for LES configurations, at the edge of the confluence zone. According to Figure 6(a), the mean surface pressure profiles produced by all three numerical simulations are reasonably similar to the corresponding profiles estimated based on experimental measurements. On the other hand, the results from WRLES of the vortex of swirl ratio 0.65 matches the experimental results much better than the results from WMLES of the same vortex.

Figure 6(b) shows the radial profiles of the standard deviation $\sigma_p / \left|\overline{P}_{\min}\right|$ of the surface pressures from the numerical simulations and experiments. The differences in the performances of the

WMLES and WRLES are remarkable. It is seen that inside the core of the vortex, the standard deviation of the surface pressure generated by WRLES matches the data from the experiments. By contrast, the radial profiles based on data from the WMLES differs significantly from the experimental data in the same region. The overprediction in both WMLES cases suggests that the wall model cannot accurately reproduce the turbulent stress distribution for tornado flows, leading to excessive unsteady forcing of the near-surface pressure field. It is also observed, however that the numerical results, whether from WRLES or WMLES, substantially underpredict the experimental measurement in regions far outside the core of the vortex. This is likely attributable to a combination of factors, including that coarser grid resolution in the outer region increases SGS dissipation and suppresses resolved fluctuation energy (Cao et al, 2018), and that the absence of resolved turbulent eddies in the prescribed inflow boundary condition removes a physical source of outer-region pressure variance (Bryan et al, 2017).

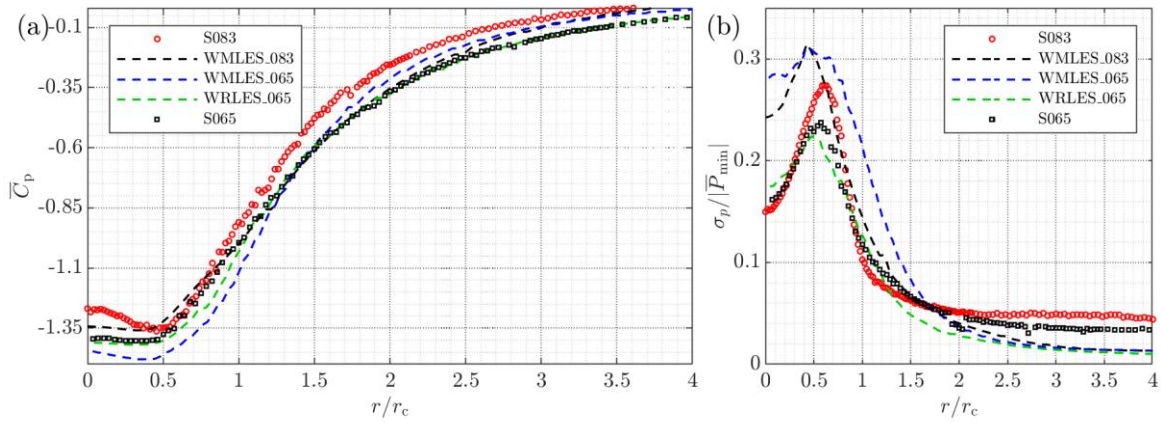

Figure 6: Comparison of radial profiles of surface pressure coefficient resulting from numerical simulations and experimental measurements: (a) Mean value and (b) standard deviation of surface pressure coefficient.

The limitations of WMLES observed in this study are closely tied to the breakdown of the equilibrium assumption inherent in standard wall models. In tornado-like vortices, the near-ground flow is subjected to strong adverse pressure gradients and significant streamline curvature, particularly near the vortex core. These effects disrupt the local balance between turbulence production and dissipation that equilibrium wall functions rely on. As a result, the wall model cannot accurately represent the near-surface shear stress, leading to errors in the predicted velocity fluctuations and surface pressure fields. By contrast, WRLES resolves these near-wall processes directly and is therefore better able to capture the complex interaction between pressure gradients, curvature, and turbulence.

4. CONCLUSION

In this study, WMLES with an equilibrium wall function and WRLES are used to numerically reproduce tornado-like vortices generated in a Ward-type tornado. A number of characteristics of mean flow field and turbulence of the numerically simulated vortices are compared with the corresponding characteristics of the physically generated vortices. In addition, some mean and fluctuating characteristics of the surface pressure of the numerically simulated vortices are also

compared with the corresponding characteristics of the surface pressure of the physically generated vortices by the tornado simulator.

The outcomes of the comparisons suggests that the WRLES outperforms the WMLES with an equilibrium wall function in reproducing the characteristics of the target physically generated vortices. The performances of these two types of LES differ in their ability to reproduce the mean and turbulent characteristic of the velocity fields of the vortices and the mean and fluctuating characteristics of the surface pressure caused by the vortices. In reproducing the mean characteristics, while the WRLES offers superior performance, the reproductions by the WMLES with an equilibrium wall also closely match the experimental measurements. By contrast, while the WRLES can reproduce the fluctuating characteristics with reasonable accuracy, the WMLES with an equilibrium wall function falls short in reproducing these characteristics. This demonstrates the limitation of WMLES with an equilibrium wall function for simulation of tornado-like vortices.

REFERENCES

Bose, S.T., Park, G.I., 2018. Wall-modeled large-eddy simulation for complex turbulent flows. Annual review of fluid mechanics 50, 535–561. https://doi.org/10.1146/annurev-fluid-122316-045241

Bryan, G.H., Dahl, N.A., Nolan, D.S., Rotunno, R., 2017. An eddy injection method for large-eddy simulations of tornado-like vortices. Monthly Weather Review 145, 1937–1961.https://doi.org/10.1175/MWR-D-16-0339.1

Cao, S., Wang, M., Cao, J., 2018. Numerical study of wind pressure on low-rise buildings induced by tornado-like flows. Journal of Wind Engineering and Industrial Aerodynamics 183, 214–222.https://doi.org/10.1016/j.jweia.2018.10.023

Chen, Q., Tang, Z., Wu, X., Zuo, D., James, D., 2023. Laboratory study of tornado-like loading on a low-rise building model. Journal of Wind Engineering and Industrial Aerodynamics 238, 105443

Gairola, A., Bitsuamlak, G., 2019. Numerical tornado modeling for common interpretation of experimental simulators. Journal of Wind Engineering and Industrial Aerodynamics 186, 32–48.https://doi.org/10.1016/j.jweia.2018.12.013

Gairola, A., Bitsuamlak, G.T., Hangan, H.M., 2024. The effect of swirl ratio and surface roughness on the boundary layer of “tornado-like” vortices. Journal of Wind Engineering and Industrial Aerodynamics 252, 105841.https://doi.org/10.1016/j.jweia.2024.105841

Haan Jr, F., Balaramudu, V.K., Sarkar, P., 2010. Tornado-induced wind loads on a low-rise building. Journal of structural engineering 136, 106–116.https://doi.org/10.1061/(ASCE)ST.1943-541X.0000093

Ishihara, T., Oh, S., Tokuyama, Y., 2011. Numerical study on flow fields of tornado-like vortices using the LES turbulence model. Journal of Wind Engineering and Industrial Aerodynamics 99, 239–248.https://doi.org/10.1016/j.jweia.2011.01.014

Kuai, L., Haan Jr, F.L., Gallus Jr, W.A., Sarkar, P.P., 2008. CFD simulations of the flow field of a laboratory-simulated tornado for parameter sensitivity studies and comparison with field measurements. Wind and Structures 11, 75–96.https://doi.org/10.12989/was.2008.11.2.075

Liu, Z., Cao, S., Liu, H., Hua, X., Ishihara, T., 2020. Effects of Reynolds number in the range from 1.6× 103 to 1.6× 106 on the flow fields in tornado-like vortices by LES: a systematical study. Journal of Wind Engineering and Industrial Aerodynamics 196, 104028.https://doi.org/10.1016/j.jweia.2019.104028

Spalding, D.B., 1961. A single formula for the law of the wall. J. Appl. Mech 28, 455–458.https://doi.org/10.1115/1.3641728

Tang, Z., Chen, Q., Wu, X., James, D.L., Zuo, D., 2025. An investigation of the major characteristics of surface pressure fields beneath two types of tornado-like vortices and their causes. Experiments in Fluids 66, 171.10.1007/s00348-025-04099-6

Tang, Z., Feng, C., Wu, L., Zuo, D., James, D.L., 2018. Characteristics of tornado-like vortices simulated in a large-scale ward-type simulator. Boundary-layer meteorology 166, 327–350.https://doi.org/10.1007/s10546-017-0305-7

Wang, A., Pan, Y., Bryan, G.H., Markowski, P.M., 2023. Modeling near-surface turbulence in large-eddy simulations of a tornado: An application of thin boundary layer equations. Monthly Weather Review 151, 1587–1607